Enhancement of spectral resolution and optical rejection ratio of Brillouin optical spectral analysis using polarization pulling

Stefan Preussler,[1] Avi Zadok,[2,*] Andrzej Wiatrek,[1] Moshe Tur,[3] and Thomas Schneider[1]

[1]*Institut für Hochfrequenztechnik, Hochschule für Telekommunikation, D-04277 Leipzig, Germany*
[2]*Faculty of Engineering, Bar-Ilan University, Ramat-Gan 52900, Israel*
[3]*School of Electrical Engineering, Faculty of Engineering, Tel-Aviv University, Tel-Aviv 69978, Israel*
[*]*Avinoam.Zadok@biu.ac.il*

Abstract: High-resolution, wide-bandwidth optical spectrum analysis is essential to the measuring and monitoring of advanced optical, millimeter-wave, and terahertz communication systems, sensing applications and device characterization. One category of high-resolution spectrum analyzers reconstructs the power spectral density of a signal under test by scanning a Brillouin gain line across its spectral extent. In this work, we enhance both the resolution and the optical rejection ratio of such Brillouin-based spectrometers using a combination of two techniques. First, two Brillouin loss lines are superimposed upon a central Brillouin gain to reduce its bandwidth. Second, the vector attributes of stimulated Brillouin scattering amplification in standard, weakly birefringent fibers are used to change the signal state of polarization, and a judiciously aligned output polarizer discriminates between amplified and un-amplified spectral contents. A frequency resolution of 3 MHz, or eight orders of magnitude below the central optical frequency, is experimentally demonstrated. In addition, a weak spectral component is resolved in the presence of a strong adjacent signal, which is 30 dB stronger and detuned by only 60 MHz. The measurement method involves low-bandwidth direct detection, and does not require heterodyne beating. The measurement range of the proposed method is scalable to cover the C + L bands, depending on the tunable pump source. The accuracy of the measurements requires that the pump frequencies are well calibrated.

OCIS codes: (290.5900) Scattering, stimulated Brillouin; (120.6200) Spectrometers and spectroscopic instrumentation; (060.4370) Nonlinear optics, fibers.

References and links

1. Y. Ma, Q. Yang, Y. Tang, S. Chen, and W. Shieh, "1-Tb/s single-channel coherent optical OFDM transmission over 600-km SSMF fiber with subwavelength bandwidth access," Opt. Express **17**(11), 9421–9427 (2009).
2. D. Hillerkuss, R. Schmogrow, T. Schellinger, M. Jordan, M. Winter, G. Huber, T. Vallaitis, R. Bonk, P. Kleinow, F. Frey, M. Roeger, S. Koenig, A. Ludwig, A. Marculescu, J. Li, M. Hoh, M. Dreschmann, J. Meyer, S. Ben Ezra, N. Narkiss, B. Nebendahl, F. Parmigiani, P. Petropoulos, B. Resan, A. Oehler, K. Weingarten, T. Ellermeyer, J. Lutz, M. Moeller, M. Huebner, J. Becker, C. Koos, W. Freude, and J. Leuthold, "26 Tbit s^{-1} line-rate super-channel transmission utilizing all-optical fast Fourier transform processing," Nat. Photonics **5**(6), 364–371 (2011).
3. T. Kuri, H. Toda, J. Olmos, and K. Kitayama, "Reconfigurable dense wavelength-division-multiplexing millimeter-waveband radio-over-fiber access system technologies," J. Lightwave Technol. **28**(16), 2247–2257 (2010).
4. C. S. Park, Y. K. Yeo, and L. C. Ong, "Demonstration of the GbE service in the converged radio-over-fiber/optical networks," J. Lightwave Technol. **28**(16), 2307–2314 (2010).
5. I. Kallfass, J. Antes, T. Schneider, F. Kurz, D. Lopez-Diaz, S. Diebold, H. Massler, A. Leuther, and A. Tessmann, "All active MMIC-based wireless communication at 220 GHz," IEEE Trans. THz Sci. Technol. **1**(2), 477–487 (2011).

#165286 - $15.00 USD Received 23 Mar 2012; revised 10 May 2012; accepted 12 May 2012; published 15 Jun 2012

6. T. Schneider, A. Wiatrek, S. Preußler, M. Grigat, and R.-P. Braun, "Link budget analysis for terahertz fixed wireless links," IEEE Trans. THz Sci. Technol. (submitted).
7. I. M. White and X. Fan, "On the performance quantification of resonant refractive index sensors," Opt. Express **16**(2), 1020–1028 (2008).
8. A. M. Armani, R. P. Kulkarni, S. E. Fraser, R. C. Flagan, and K. J. Vahala, "Label-free, single-molecule detection with optical microcavities," Science **317**(5839), 783–787 (2007).
9. D. M. Baney, B. Szafraniec, and A. Motamedi, "Coherent optical spectrum analyzer," IEEE Photon. Technol. Lett. **14**(3), 355–357 (2002).
10. F. R. Giorgetta, I. Coddington, E. Baumann, W. C. Swann, and N. R. Newbury, "Fast high resolution spectroscopy of dynamic continuous-wave laser sources," Nat. Photonics **4**(12), 853–857 (2010).
11. J. M. S. Domingo, J. Pelayo, F. Villuendas, C. D. Heras, and E. Pellejer, "Very high resolution optical spectrometry by stimulated Brillouin scattering," IEEE Photon. Technol. Lett. **17**(4), 855–857 (2005).
12. T. Schneider, "Wavelength and line width measurement of optical sources with femtometre resolution," Electron. Lett. **41**(22), 1234–1235 (2005).
13. R. W. Boyd, *Nonlinear Optics* (Academic Press, 2008).
14. A. Yeniay, J. Delavaux, and J. Toulouse, "Spontaneous and stimulated Brillouin scattering gain spectra in optical fibers," J. Lightwave Technol. **20**(8), 1425–1432 (2002).
15. S. M. Foaleng, M. Tur, J.-C. Beugnot, and L. Thevenaz, "High spatial and spectral resolution long range sensing using Brillouin echos," J. Lightwave Technol. **28**(20), 2993–3003 (2010).
16. S. Preußler, A. Wiatrek, K. Jamshidi, and T. Schneider, "Brillouin scattering gain bandwidth reduction down to 3.4MHz," Opt. Express **19**(9), 8565–8570 (2011).
17. S. Preußler, A. Wiatrek, K. Jamshidi, and T. Schneider, "Ultrahigh-resolution spectroscopy based on the bandwidth reduction of stimulated Brillouin scattering," IEEE Photon. Technol. Lett. **23**(16), 1118–1120 (2011).
18. F. Mihélic, D. Bacquet, J. Zemmouri, and P. Szriftgiser, "Ultrahigh resolution spectral analysis based on a Brillouin fiber laser," Opt. Lett. **35**(3), 432–434 (2010).
19. A. Zadok, E. Zilka, A. Eyal, L. Thévenaz, and M. Tur, "Vector analysis of stimulated Brillouin scattering amplification in standard single-mode fibers," Opt. Express **16**(26), 21692–21707 (2008).
20. A. Wise, M. Tur, and A. Zadok, "Sharp tunable optical filters based on the polarization attributes of stimulated Brillouin scattering," Opt. Express **19**(22), 21945–21955 (2011).
21. A. Galtarossa, L. Palmieri, M. Santagiustina, L. Schenato, and L. Ursini, "Polarized Brillouin amplification in randomly birefringent and unidirectionally spun fibers," Photon. Technol. Lett. **20**(16), 1420–1422 (2008).
22. L. Ursini, M. Santagiustina, and L. Palmieri, "Polarization-dependent Brillouin gain in randomly birefringent fibers," IEEE Photon. Technol. Lett. **22**(10), 712–714 (2010).
23. L. Thévenaz, "Slow and fast light in optical fibers," Nat. Photonics **2**(8), 474–481 (2008).
24. Z. Zhu, D. J. Gauthier, Y. Okawachi, J. E. Sharping, A. L. Gaeta, R. W. Boyd, and A. E. Willner, "Numerical study of all-optical slow light delays via stimulated Brillouin scattering in an optical fiber," J. Opt. Soc. Am. B **22**(11), 2378–2384 (2005).
25. A. Zadok, S. Chin, L. Thévenaz, E. Zilka, A. Eyal, and M. Tur, "Polarization-induced distortion in stimulated Brillouin scattering slow-light systems," Opt. Lett. **34**(16), 2530–2532 (2009).
26. T. Schneider, R. Henker, K.-U. Lauterbach, and M. Junker, "Comparison of delay enhancement mechanisms for SBS-based slow light systems," Opt. Express **15**(15), 9606–9613 (2007).
27. M. O. van Deventer and J. Boot, "Polarization properties of stimulated Brillouin scattering in single mode fibers," J. Lightwave Technol. **12**(4), 585–590 (1994).
28. J. P. Gordon and H. Kogelnik, "PMD fundamentals: polarization mode dispersion in optical fibers," Proc. Natl. Acad. Sci. U.S.A. **97**(9), 4541–4550 (2000).
29. A. Voskoboinik, J. Wang, B. Shamee, S. R. Nuccio, L. Zhang, M. Chitgarha, A. E. Willner, and M. Tur, "SBS-based fiber optical sensing using frequency-domain simultaneous tone interrogation," J. Lightwave Technol. **29**(11), 1729–1735 (2011).
30. Z. Shmilovitch, N. Primerov, A. Zadok, A. Eyal, S. Chin, L. Thevenaz, and M. Tur, "Dual-pump push-pull polarization control using stimulated Brillouin scattering," Opt. Express **19**(27), 25873–25880 (2011).
31. Z. W. Barber, W. R. Babbitt, B. Kaylor, R. R. Reibel, and P. A. Roos, "Accuracy of active chirp linearization for broadband frequency modulated continuous wave lidar," Appl. Opt. **49**(2), 213–219 (2010).
32. P. Del'Haye, O. Arcizet, M. L. Gorodetsky, R. Holzwarth, and T. J. Kippenberg, "Frequency comb assisted diode laser spectroscopy for measurement of microcavity dispersion," Nat. Photonics **3**(9), 529–533 (2009).
33. M. Sagues and A. Loayssa, "Orthogonally polarized optical single sideband modulation for microwave photonics processing using stimulated Brillouin scattering," Opt. Express **18**(22), 22906–22914 (2010).
34. T. Schneider, K. Jamshidi, and S. Preußler, "Quasi-light Storage: a method for the tunable storage of optical packets with a potential delay-bandwidth product of several thousand bits," J. Lightwave Technol. **28**(17), 2586–2592 (2010).
35. S. Preußler, K. Jamshidi, A. Wiatrek, R. Henker, C.-A. Bunge, and T. Schneider, "Quasi-light-storage based on time-frequency coherence," Opt. Express **17**(18), 15790–15798 (2009).

#165286 - $15.00 USD Received 23 Mar 2012; revised 10 May 2012; accepted 12 May 2012; published 15 Jun 2012

1. Introduction

The acquisition of optical power spectral densities (PSDs) is among the most fundamental and widely practiced procedures in optical test and measurement. Optical spectrum analyzers (OSAs) are routinely employed in the monitoring of optical communication networks, in the readout of variety of optical sensors, and in the characterization of the transfer functions of passive and active photonic devices. A primary figure of merit of OSAs is their spectral resolution. Traditional, diffraction grating-based OSAs provide a spectral resolution on the order of 1 GHz. In recent years, such resolution is increasingly becoming insufficient. For example, spectrally efficient, modern optical communication formats, such as optical orthogonal frequency domain multiplexing (O-OFDM), make use of a large number of sub-carrier tones that are densely packed [1, 2]. The frequency separation between adjacent sub-carriers may be as small as a few tens of MHz [1], hence the monitoring of such signals would benefit from an OSA of comparable resolution. Similarly, a high resolution, wideband OSA would be instrumental in the characterization of dense radio-over-fiber transmission links [3, 4] and for millimeter-wave [5] or terahertz communication systems [6]. Last but not least, a high resolution OSA would also help identify miniscule variations in the transfer function of resonant photonic devices [7, 8], and thereby facilitate extremely sensitive environmental monitoring [7, 8].

An arbitrarily high spectral resolution may be obtained, at least in principle, through heterodyne interference of a signal under test with a local oscillator and subsequent radio-frequency (RF) spectral analysis [9, 10]. The practical realization of such coherent OSAs is often challenging, as they may require highly stable and low-noise local oscillators, optical phase-locked loops or frequency comb sources [9, 10], and so on. Measurement techniques which employ direct detection are in general simpler to implement. Additionally, the usable spectral measurement range of coherent OSAs is sometimes restricted by the bandwidth of the subsequent RF spectrum analyzer and that of the photo diode, which are on the order of several tens of GHz. For ultra-wideband optical systems this measurement range might not be enough.

Over the last decade, high-resolution OSAs based on stimulated Brillouin scattering (SBS) amplification were proposed and demonstrated [11, 12]. In an SBS-OSA, a pump wave and the signal under test counter-propagate along an optical fiber. The pump wave introduces a relatively narrow spectral window of signal wave amplification, whose central frequency is offset from that of the pump itself by the Brillouin shift of the fiber Ω_B, which is approximately $2\pi\cdot 11$ GHz [13]. When the pump is sufficiently strong, the overall signal power at the fiber output is dominated by the contribution of amplified spectral components that fall within the SBS gain window. Hence the signal PSD can be reconstructed through scanning the frequency of the pump wave [11, 12]. The fundamental resolution of this technique is restricted by the Brillouin bandwidth Γ_B, which is on the order of $2\pi\cdot 20$ MHz to $2\pi\cdot 30$ MHz in standard fibers at 1550 nm wavelengths [13–15]. Use of an intense pump wave could reduce the Brillouin bandwidth towards 10 MHz [14]. SBS-OSAs are prone, however, to cross-talk from out-of-band spectral contents. Signal components outside the SBS gain window, although unamplified, propagate to the output with little loss, and thereby deteriorate the close-in dynamic range (or optical rejection ratio), which signifies the ability to recognize a weak spectral component in the presence of a second, stronger one at a closely spaced frequency.

Recently, it has been shown that the resolution of SBS-OSAs can be enhanced through careful synthesis of the Brillouin gain line. Preussler and co-authors had used a superposition of three Brillouin pumps: one for introducing a gain line, and two others to generate Brillouin loss lines whose central frequencies were detuned from that of the gain line by approximately $\pm\ 0.5\Gamma_B$ [16, 17]. The bandwidth of the composite SBS line-shape was reduced to 3.4 MHz [16], however the resolution of their SBS-OSA could only be improved to 8 MHz [17]. In

#165286 - $15.00 USD Received 23 Mar 2012; revised 10 May 2012; accepted 12 May 2012; published 15 Jun 2012

another study, the signal under test was used as a pump source for an ultra-narrow Brillouin fiber laser [18]. Heterodyne beating between the Brillouin fiber laser and the original signal yielded spectral measurements with a frequency resolution on a kHz scale [18]. The spectral range of the measurement, however, was restricted to approximately 10 MHz.

In this work, we reduce the linewidth and simultaneously improve the optical rejection ratio of a straight-forward, scalar SBS amplification process, using the polarimetric attributes of SBS in standard, weakly birefringent fibers. A vector analysis of SBS had revealed that the state of polarization (SOP) of the amplified signal is drawn towards a particular state, which is governed by the SOP of the pump [19–22]. That particular state can be made different from the output polarization of unamplified, out-of-band signal components, unaffected by SBS [19, 20]. Based on this principle, an output polarizer is used to reject the unamplified spectral components, while those within the SBS bandwidth are partially transmitted [20]. Using this technique, a spectral resolution of 3 MHz is obtained, using a modest pump power level below 10 mW. The resolution of a scalar SBS amplification using the same pump power is an order of magnitude lower. At the same time, an optical rejection ratio of 30 dB, for a frequency separation of only 60 MHz, is demonstrated as well. The corresponding ratio of a scalar SBS process using the same pump power is two orders of magnitude smaller. Weak modulation sidelobes in the signal wave, that were indiscernible to the straight-forward setup, are readily observed.

2. Principle of operation

Consider the arrangement of Fig. 1. A polarized signal under test enters a section of standard optical fiber at position $z = 0$, and propagates in the positive z direction. We denote the vector electric field of the signal as $\vec{E}_{sig}\left(\omega_{sig}, z\right)$, where ω_{sig} is an optical frequency variable.

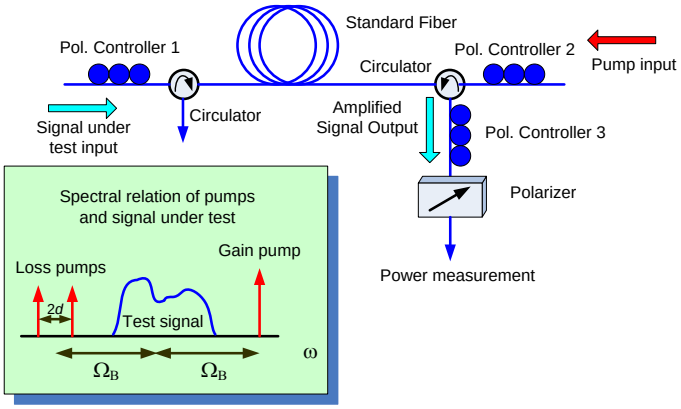

Fig. 1. Schematic illustration of a polarization-enhanced SBS-OSA arrangement. Relative frequencies of pump components and the signal under test are shown in the inset box.

A relatively intense, polarized Brillouin pump wave is launched at the opposite end of the fiber at $z = L$, with L the fiber length, and counter-propagates in the negative z direction. The interaction between the pump wave and the test signal may give rise to SBS amplification of the latter [13, 14]. We denote the complex-valued, exponential gain coefficient of SBS as $g\left(\omega_{sig}\right)$, in units of m^{-1}. The functional form of $g\left(\omega_{sig}\right)$ is generally given by a convolution of the inherent Lorentzian line shape of SBS with the PSD of the pump wave [23, 24]. Specific shapes of the gain coefficient used in this work will be detailed later in this section.

In propagation along the fiber, the signal under test is subject to both SBS amplification and weak, residual birefringence that is randomly changing its SOP. The pump wave, on the

#165286 - $15.00 USD Received 23 Mar 2012; revised 10 May 2012; accepted 12 May 2012; published 15 Jun 2012

other hand, is assumed to be sufficiently strong so that it is undepleted, and therefore propagates subject to birefringence alone. Previous studies had formulated and analyzed the coupled, vector propagation equations of the two waves, and had reached several observations, which were also supported experimentally [19, 20]: For a given launch SOP of the pump wave, the complex magnitude gain of the signal varies with its own input SOP, ranging between maximum and minimum values. For L longer than a few hundred meters, these maximum and minimum gain values are $G_{\max}\left(\omega_{sig}\right)=\exp\left[\frac{1}{3}g\left(\omega_{sig}\right)L\right]$ and $G_{\min}\left(\omega_{sig}\right)=\exp\left[\frac{1}{6}g\left(\omega_{sig}\right)L\right]$, respectively [19]. The maximum and minimum gain values are associated with a pair of orthogonal input SOPs of the signal. We denote the unit Jones vectors if these SOPs as $\hat{e}_{\max}^{in}$ and $\hat{e}_{\min}^{in}$, respectively. The two gain values also correspond to two orthogonal SOPs of the output, amplified signal: $\hat{e}_{\max}^{out}$ and $\hat{e}_{\min}^{out}$, respectively. The above input and output SOPs are governed by the SOP of the pump, and are largely independent of ω_{sig} within the SBS bandwidth [25].

An arbitrarily polarized input signal may be decomposed in the basis of $\hat{e}_{\max}^{in}$ and $\hat{e}_{\min}^{in}$:

$$\vec{E}\left(\omega_{sig},z=0\right)=E_0\left(\omega_{sig}\right)\left(a\hat{e}_{\max}^{in}+b\hat{e}_{\min}^{in}\right). \tag{1}$$

Here, $E_0\left(\omega_{sig}\right)$ is a scalar, frequency-dependent complex magnitude and $|a|^2+|b|^2=1$. The corresponding output signal vector takes the following form [20]:

$$\vec{E}\left(\omega_{sig},z=L\right)=E_0\left(\omega_{sig}\right)\left[aG_{\max}\left(\omega_{sig}\right)\hat{e}_{\max}^{out}+bG_{\min}\left(\omega_{sig}\right)\hat{e}_{\min}^{out}\right]. \tag{2}$$

Since the maximum and minimum SBS magnitude gains vary with ω_{sig}, the output signal SOP is frequency dependent as well. As typically $G_{\max}\left(\omega_{sig}\right)>>G_{\min}\left(\omega_{sig}\right)$, the output SOP of SBS-amplified signal components is being drawn towards a particular state, that of $\hat{e}_{\max}^{out}$, unless *a* is vanishingly small. The phenomenon is referred to as *polarization pulling* [19–22, 25]. In particular, the SOP of amplified spectral components of the signal under test may differ substantially from that of out-of-band, unamplified components (for which $G_{\max}\left(\omega_{sig}\right)=G_{\min}\left(\omega_{sig}\right)=1$). We use this polarization distinction in order to further discriminate between amplified and unamplified spectral components, and enhance the resolution and optical rejection ratio of the SBS-OSA.

Consider next a polarizer at the signal output end of the fiber. The transmission axis of the polarizer is aligned with an SOP whose unit Jones vector is $\hat{p}=p_{\max}\hat{e}_{\max}^{out}+p_{\min}\hat{e}_{\min}^{out}$, with $|p_{\max}|^2+|p_{\min}|^2=1$. The PSD of the output signal following the polarizer becomes [20]:

$$\left|\vec{E}^{out}\left(\omega_{sig}\right)\right|^2=\left|E_0\left(\omega_{sig}\right)\right|^2\left|ap_{\max}^{*}G_{\max}\left(\omega_{sig}\right)+bp_{\min}^{*}G_{\min}\left(\omega_{sig}\right)\right|^2. \tag{3}$$

For any given choices of launch SOPs of both pump and test signal, we have the freedom to adjust the output polarizer so that out-of-band spectral components are entirely rejected: $ap_{\max}^{*}+bp_{\min}^{*}=0$. Subject to this adjustment, the output signal PSD becomes:

$$\begin{aligned}\left|\vec{E}^{out}\left(\omega_{sig}\right)\right|^2&=\left|ap_{\max}^{*}\right|^2\left|G_{\max}\left(\omega_{sig}\right)-G_{\min}\left(\omega_{sig}\right)\right|^2\left|E_0\left(\omega_{sig}\right)\right|^2.\\&\equiv\left|H\left(\omega_{sig}\right)\right|^2\left|E_0\left(\omega_{sig}\right)\right|^2.\end{aligned} \tag{4}$$

#165286 - $15.00 USD Received 23 Mar 2012; revised 10 May 2012; accepted 12 May 2012; published 15 Jun 2012

In Eq. (4) we have defined a transfer function for the amplified signal at the output of the polarizer: $H\left(\omega_{sig}\right) \equiv ap_{\max}^{*}\left[G_{\max}\left(\omega_{sig}\right) - G_{\min}\left(\omega_{sig}\right)\right]$. Although SBS amplification is a nonlinear optical phenomenon, it is nevertheless linear in the signal wave within the undepleted pump regime [13] hence its description in terms of an equivalent frequency-domain transfer function is legitimate. The maximum value of the coefficient $\left|ap_{\max}^{*}\right|^2$, subject to the constraint of complete out-of-band rejection, is 0.25 (with $\left|a\right|^2 = \left|p_{\max}^{*}\right|^2 = \frac{1}{2}$). For a sufficiently intense pump power, and in the vicinity of the gain peak, we may approximate:

$$\left|H\left(\omega_{sig}\right)\right|^2 \approx 0.25\left|G_{\max}\left(\omega_{sig}\right)\right|^2 = 0.25\exp\left\{\tfrac{2}{3}\mathrm{Re}\left[g\left(\omega_{sig}\right)\right]L\right\}, \tag{5}$$

whereas outside the SBS amplification window $\left|H\left(\omega_{sig}\right)\right|^2 \approx 0$. This result is in marked contrast to the transmission of unamplified spectral contents in a scalar SBS amplification process, without polarization assistance, for which $\left|H\left(\omega_{sig}\right)\right|^2 \approx 1$. We may therefore expect that a polarization enhanced SBS-OSA would provide a considerably larger optical rejection ratio than that of a corresponding scalar arrangement. In addition, polarization discrimination helps reduce the spectral width of $H\left(\omega_{sig}\right)$ below that of a scalar SBS amplification window.

Let us turn now to the spectral synthesis of the SBS pump wave. Following [26], the pump wave consists of three continuous-wave components. The frequency of the first component is adjusted to $\omega_{sig}^{0} + \Omega_B$, and it introduces SBS amplification of the signal under test with maximum gain at $\omega_{sig} = \omega_{sig}^{0}$. The additional two pump wave components are of frequencies $\omega_{sig}^{0} - \Omega_B \pm d$, where d is a detuning factor on the order of Γ_B. These two components introduce SBS loss lines, with peak attenuation frequencies of $\omega_{sig}^{0} \pm d$. The three pump components are assumed to be co-polarized. The signal under test is therefore subject to a composite SBS process, comprised of a spectral gain and two spectral losses in overlap. The SBS gain coefficient of the entire process is of the form [26]:

$$\begin{aligned} g\left(\omega_{sig}\right) = {} & g_0 P\left(1 - 2j\frac{\omega_{sig} - \omega_{sig}^{0}}{\Gamma_B}\right)^{-1} - mg_0 P\left(1 - 2j\frac{\omega_{sig} - \omega_{sig}^{0} - d}{\Gamma_B}\right)^{-1} \\ & - mg_0 P\left(1 - 2j\frac{\omega_{sig} - \omega_{sig}^{0} + d}{\Gamma_B}\right)^{-1}. \end{aligned} \tag{6}$$

In Eq. (6), P denotes the power of the amplifying pump component, mP is the power of each of the two attenuating pump components, and g_0 is the peak gain coefficient of SBS per unit of pump power. In standard fibers, g_0 is on the order of 0.1 $[\mathrm{m}\cdot\mathrm{W}]^{-1}$. The two detuned loss lines largely cancel out the gain to the sides of the primary amplification peak, rendering the linewidth of the entire composite process narrower [26].

Figure 2 shows the calculated transfer function for SBS amplification of the signal under test, as a function of the frequency offset $\Delta f \equiv \left(\omega_{sig} - \omega_{sig}^{0}\right)/2\pi$. The transfer function was calculated for a three-pump process (Eq. (6), red lines), as well as for a single gain line (m = 0, black lines). The transfer function is shown for polarization-assisted processes (Eq. (4), solid lines), while that of a scalar process, $\left|H\left(\omega_{sig}\right)\right|^2 = \exp\left\{\tfrac{2}{3}\mathrm{Re}\left[g\left(\omega_{sig}\right)\right]L\right\}$, is provided for

#165286 - $15.00 USD Received 23 Mar 2012; revised 10 May 2012; accepted 12 May 2012; published 15 Jun 2012

comparison (dashed lines). The transfer function of the polarization assisted SBS processes effectively rejects the out-of-band components of the signal under test. In addition, the transfer function of the composite, three-pump process is seen to be narrower than that of a single SBS gain line and it suppresses the out-of band components even further. Compared to the corresponding scalar process, the triple-pump, polarization-assisted Brillouin amplification provides relative out-of-band suppression that is 20 dB stronger.

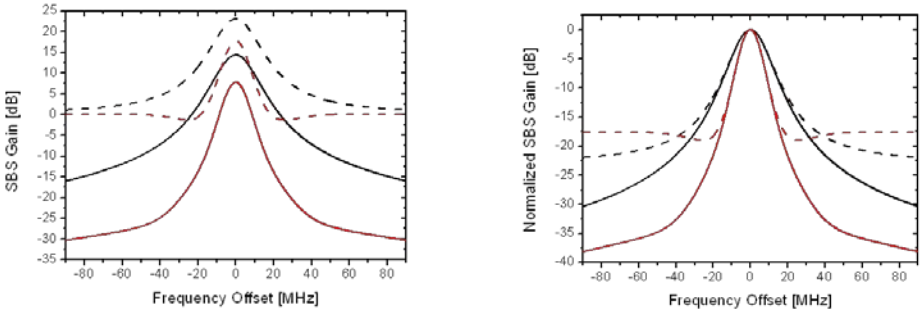

Fig. 2. Calculated SBS power amplification of a signal under test $\left|H\left(\Delta f\right)\right|^2$ (left), and the normalized power gain $\left|H\left(\Delta f\right)\right|^2 / \left|H\left(\Delta f = 0\right)\right|^2$ (right), for various processes. The simulation parameters were L = 20 km, Γ_B = 2π·40 MHz, g_0 = 0.1 [m·W]$^{-1}$. Dashed curves: scalar Brillouin amplification for a single gain line (black, P = 4 mW), and combined gain and two losses (red, P = 9 mW, m = 0.45, d = 0.3 Γ_B). Solid curves: corresponding polarization assisted SBS amplification for a single gain line (black), and combined gain and two losses (red). The polarization assisted process is seen to effectively reject the optical power of unamplified spectral components of the signal under test. This rejection is more effective when the gain is combined with two losses at its edges.

The measured power at the output of the polarizer effectively samples the power of the signal under test at $\omega_{sig} = \omega_{sig}^0$: $\left|E_0\left(\omega_{sig}^0\right)\right|^2$ (see Eq. (4) and Fig. (2)). The PSD of the signal under test can be reconstructed by sweeping the frequencies of the three pump lines together, so that their central frequency ω_{sig}^0 is scanned while the differences between their respective frequencies remain unchanged. The application of the method in a high-resolution, high rejection ratio SBS-OSA is experimentally demonstrated next.

3. Experiment and results

The experimental setup is shown in Fig. 3. A 20 km-long AllWave fiber was used as the SBS gain medium. The SBS amplifying pump was driven by an ultra-narrow fiber laser (FL) of 1550 nm wavelength and a linewidth below 2 kHz (see yellow block in Fig. 3). We denote the optical frequency of the FL as ω_p. An erbium-doped fiber amplifier (EDFA 1) and a manual polarization controller (PC 3) were used to adjust the power and SOP of the amplifying pump, respectively. The two SBS attenuating pumps were independently generated from the output of a distributed feedback (DFB) laser diode (linewidth 1 MHz), the central frequency of which was adjusted to $\omega_p - 2\Omega_B$ through careful current and temperature control. Light from the DFB output passed through a Mach-Zehnder modulator (MZM 4), which was biased to suppress the carrier wave at $\omega_p - 2\Omega_B$ and driven by a sine-wave of frequency d. The resulting dual modulation sidebands, at frequencies $\omega_p - 2\Omega_B \pm d$, were amplified by EDFA 2 and used as the SBS attenuating pumps (see blue block of Fig. 3). PC4 was used to align the

#165286 - $15.00 USD Received 23 Mar 2012; revised 10 May 2012; accepted 12 May 2012; published 15 Jun 2012

SOP of the loss pumps in parallel with that of the gain pump. The three pumps were combined by a 3 dB coupler and launched into the fiber gain medium via a fiber-optic circulator.

The SBS probe wave (signal under test) was drawn from the same FL that was also used for the gain pump generation. MZM 1 was biased to suppress the optical carrier at frequency ω_p, and was driven by a sine wave at varying frequency $\Omega \sim \Omega_B$ to generate double sidelobes of optical frequencies $\omega_p \pm \Omega$. The lower sideband was subject to potential amplification by the three-pump SBS process, depending on the choice of Ω (see insets (1) through (3) of Fig. 3 for the relative frequencies of the pump waves and the signal under test). The test signal was then modulated in two stages. First, low frequency modulation from the output of an electrical lock-in amplifier was imposed on the signal through MZM 2, in order to facilitate the eventual low-noise detection of weak optical power levels (see grey block of Fig. 3). Next, MZM 3 was used to introduce modulation sidebands, with variable magnitude and variable frequency spacing f_{mod} in the range of 3 - 30 MHz (green block of Fig. 3). These sidebands were used to assess the resolution and optical rejection ratio of the polarization-assisted SBS-OSA. Note that in our experiment, a test PSD of pre-determined shape was swept across a fixed, composite SBS gain line, through varying Ω. Although a practical SBS-OSA would work in the opposite manner, with the signal PSD held fixed and the frequencies of the pumps being swept, the chosen arrangement was more readily accessible within our equipment constraints, and is nevertheless equivalent in terms of dynamic range and resolution.

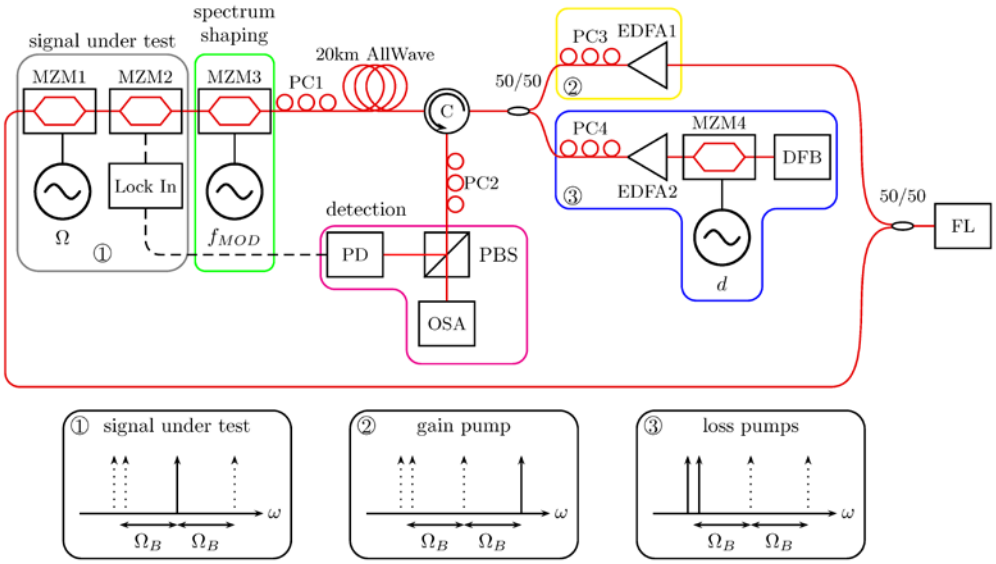

Fig. 3. An experimental setup for the realization of an ultra-high resolution optical spectrum analyzer. The grey block implements a scanning of the central frequency of a signal under test; the green block introduces modulation sidebands to the signal under test; the SBS gain pump is generated in the yellow block, whereas the two SBS loss pumps are generated in the blue block. The magenta block describes the detection scheme. Insets (1) through (3) denote the relative frequencies of the signal under test, the amplifying Brillouin pump and the attenuating Brillouin pumps, respectively. FL: narrow linewidth fiber laser, DFB: distributed feedback laser diode, MZM: Mach-Zehnder modulator, EDFA: erbium doped fiber amplifier, PC: polarization controller, C: circulator, PBS: polarization beam splitter, PD: photo diode, OSA: commercial optical spectrum analyzer used for monitoring the experiment.

Following the multiple modulation stages, the test signal was directed into the fiber gain medium from the end opposite that of the pumps launch. The SOP of the test signal at its

#165286 - $15.00 USD Received 23 Mar 2012; revised 10 May 2012; accepted 12 May 2012; published 15 Jun 2012

input end of the fiber was adjusted using PC 1. Following propagation in the fiber, the output signal under test passed through PC 2 and a polarization beam splitter (PBS), operating together as an output polarizer of adjustable state. The output power of the signal under test was measured by a photo-diode (PD), and connected to the input port of the lock-in amplifier (see magenta block of Fig. 3). A commercial OSA was connected to the complementary output of the PBS for monitoring the experiment.

Special attention was given to the relative alignment of the multiple PCs, in accord with the considerations of the previous section. The launch SOPs of all three pumps (PC 3, PC 4) were co-aligned along an arbitrary state, and held fixed for the entire duration of the experiment. For initial calibration, the input signal was disconnected, and the amplified spontaneous Brillouin scattering emission was observed at the signal output end. The SOP of the spontaneous Brillouin scattering is known to be aligned with $\hat{e}_{\max}^{out}$ [19, 27]. First $\hat{e}_{\max}^{out}$ was identified by setting PC 2 to maximum transmission of the spontaneous Brillouin scattering through to the PD, and the output power was noted. Then, PC 2 was readjusted until the transmitted power of the spontaneous Brillouin scattering was reduced by 50%, signifying $\left|p_{\max}^{*}\right|^2 = \frac{1}{2}$. Lastly, Ω was detuned temporarily by several times Γ_B, the test signal was reintroduced, and PC 1 was used to adjust the test signal input SOP until the output signal was entirely blocked by the PBS in the absence of SBS amplification. This final adjustment guaranteed that $ap_{\max}^{*} + bp_{\min}^{*} = 0$, as necessary.

Experiments with a single amplifying pump were carried out with EDFA 1 tuned to an output power of 4 mW. In triple-pump experiments, the power of the amplifying pump was raised to 9 mW, and that of each of the two attenuating pumps was set to 4 mW. The extent of polarization pulling is governed by the integrated amplification over the length of the fiber. While higher pump power levels were used in our earlier work [19], the fiber used was an order of magnitude shorter. As shown in the preceding section, significant polarization pulling is expected with the above pump power levels and the given fiber length. The frequency separation $2d$ between the two attenuating pumps was $2\pi \cdot 16$ MHz.

In the first set of measurements, the spectral shape and width of the SBS processes were characterized. To that end, the modulation of MZM 3 at frequency f_{mod} was disconnected. Figure 4 shows the obtained gain spectra for several configurations. The full width at half maximum (FWHM) of a scalar SBS process with a single amplifying pump, subject to the experimental parameters, was 40 MHz (black curve). The maximum gain of a single-pump, polarization assisted process was slightly lowered, however its bandwidth was reduced to around 20 MHz (red curve). Even more importantly, the spectral components in the vicinity of the SBS gain line were sharply cut off: The relative power gain at spectral detuning of 20 and 30 MHz was −10 dB and −20 dB, respectively. For detuning of more than 43 MHz from the line centre, the spectral components of the signal were suppressed below the detection threshold of the lock-in amplifier. The introduction of the two attenuating SBS pumps, alongside polarization discrimination, lowered the gain for the composite SBS process by 15 dB. However, the gain bandwidth was reduced to around 3 MHz. The dynamic range of the measurements was restricted by that of the lock-in amplifier.

#165286 - $15.00 USD Received 23 Mar 2012; revised 10 May 2012; accepted 12 May 2012; published 15 Jun 2012

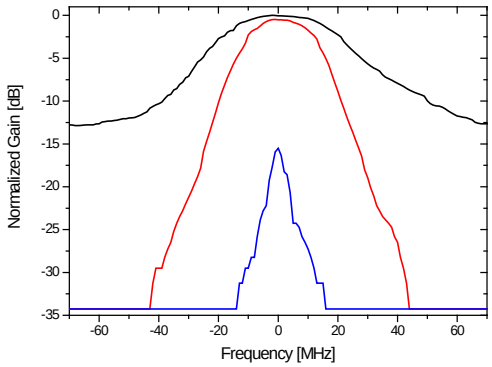

Fig. 4. Measured normalized gain of several SBS processes as a function of the detuning of the probe wave from its frequency of maximum amplification. A 20-km long standard fiber was used as the SBS gain medium. Black: a scalar process with a single amplifying pump, P = 4 mW. Red: a polarization-enhanced process with a single amplifying pump. Blue: a composite process comprised of a central gain line and two losses, with polarization enhancement, P = 9 mW, m = 0.45, $d = 2\pi \cdot 8$ MHz. A carefully adjusted output polarizer reduces the SBS gain marginally, but at the same time suppresses the unamplified spectral components of the signal and leads to a bandwidth reduction of around 50% (red). With two loss lines to the sides of the gain line, the bandwidth can be reduced by more than an order of magnitude. However, the SBS amplification is reduced by about 15 dB (blue).

Figure 5 shows SBS-OSA measurement of several test signal patterns, using polarization enhancement and a single amplifying pump. An example of a spectrum obtained with the corresponding scalar SBS process is provided for comparison. In all experiments, MZM 3 was driven by sine waves of frequency f_{mod} = 30 MHz, with a varying voltage magnitude, to generate modulation sidelobes. A scalar SBS-OSA at the given pump power could barely resolve even the first-order modulation sidelobes at ± f_{mod}. The optical rejection ratio of a spectral component detuned by 60 MHz was only 9 dB (black curve). When polarization enhancement was employed, on the other hand, the first-order sidebands were clearly distinguishable from the test signal carrier, and the second order sidebands were visible as well. Even for a very low modulation voltage of just $0.04V_{\pi}$ the second order sidebands, which are 60 MHz away from the carrier and around 30 dB lower, could still be resolved.

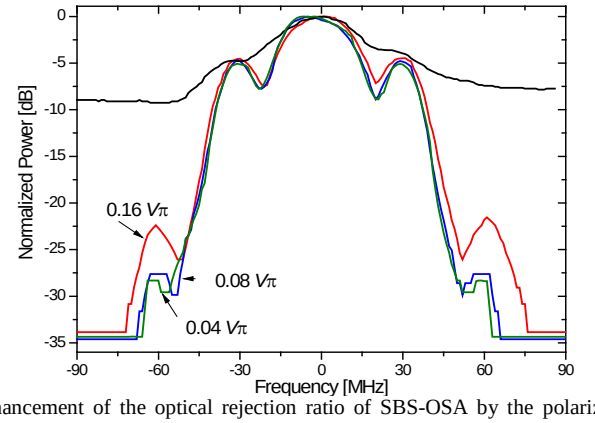

Fig. 5. Enhancement of the optical rejection ratio of SBS-OSA by the polarization pulling effect. The signal under test was modulated by a 30 MHz sine wave. Blue, red and green curves correspond to polarization-enhanced measurements of signals that were modulated using different RF power levels. A single amplifying pump was used, P = 9 mW. Black: an example of a corresponding measurement using a scalar SBS-OSA. By virtue of polarization pulling, the optical rejection ratio is considerably improved, and spectral components 30 dB lower than the maximum level are clearly visible.

#165286 - $15.00 USD Received 23 Mar 2012; revised 10 May 2012; accepted 12 May 2012; published 15 Jun 2012

Spectral measurements obtained with polarization pulling in conjunction with a bandwidth-reduced, composite SBS process are provided in Fig. 6. Here f_{mod} was varied from 10 MHz down to 3 MHz. The inset shows the 10 MHz and 7 MHz spectra on a logarithmic scale. Even for a modulation frequency of as low as 3 MHz, the different sidebands in the test signal spectrum are clearly distinguishable.

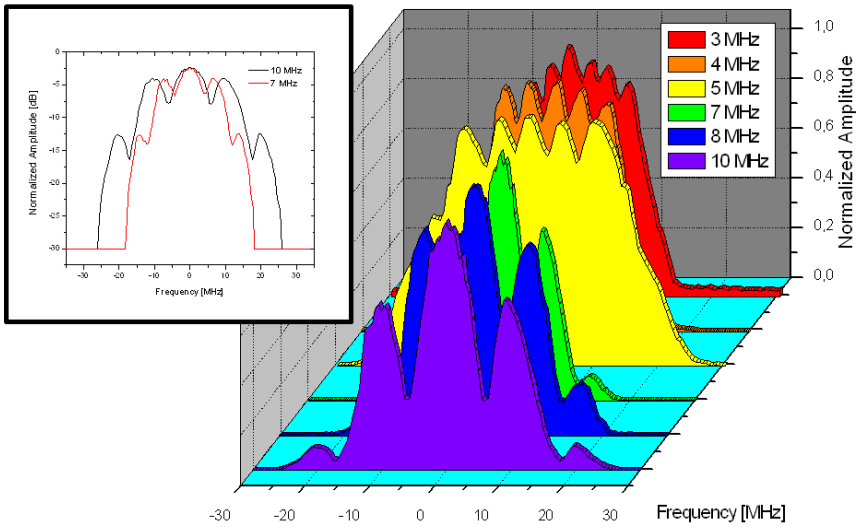

Fig. 6. Normalized, measured spectra of amplitude-modulated signals under test, on a linear scale. The modulation frequency was changed from 10 MHz down to 3 MHz. The inset shows the normalized, measured spectra for modulation frequencies of 10 and 7 MHz in a logarithmic scale. The drive voltage to the MZM had to be modified for different modulation rates due to limitations of the particular device, hence the inconsistent spectral shape.

4. Discussion and conclusions

In this work we have proposed and demonstrated a method for improving the resolution and optical rejection ratio of Brillouin-based spectral analysis, based on the vector propagation properties of SBS in standard, weakly birefringent fibers. The spectral measurement range of the scheme involving superimposed Brillouin gain-and-loss lines would be restricted to the order of $2\Omega_B$, since signal components of frequencies Ω_B below those of the loss pumps would be amplified and polarization-pulled as well. However, a standard tunable optical filter can be added to suppress widely detuned spectral components. The measurement range of a polarization-enhanced, single-pump process, on the other hand, would only be limited eventually by polarization mode dispersion (PMD) in the fiber gain medium [28]. PMD could prevent the complete rejection of signal components that are widely detuned from the SBS gain peak. The differential group delay associated with PMD in standard fibers that are a few km long is on the order of ps. Therefore, measurement ranges approaching the THz scale are feasible. The detrimental effect of PMD can be reduced if the signal under test is aligned with a principal state of polarization [28], and if the alignment of polarization component is re-calibrated at several frequencies. A broad spectral measurement range would also require an adjustment of the Brillouin frequency shift Ω_B as a function of the optical frequency of the signal under test [29].

Compared with an OSA based on a straight-forward, scalar SBS process, and, for the same low pump power levels (below 10 mW), the reported method provides an order-of-magnitude improvement in resolution to 3 MHz, and two-orders-of-magnitude enhancement

#165286 - $15.00 USD Received 23 Mar 2012; revised 10 May 2012; accepted 12 May 2012; published 15 Jun 2012

of the optical rejection ratio to 30 dB (Note, though, that sophisticated scalar SBS-OSAs may reach higher resolution and rejection ratios than those obtained with the scalar setup of our experiments). One possible avenue towards better performance of scalar setups involves the use of higher pump power. However, stronger pumping would also benefit the performance of the polarization-assisted implementation, and its added value would remain. The dynamic range of GHz-resolution, grating-based OSAs, for example, could be as high as 80 dB. However, their optical rejection ratio for a detuning of several GHz is more modest, on the order of 30 dB. The method proposed in this work is particularly attractive for the test and measurement of advanced optical communication signals, and for the characterization of millimeter-wave and terahertz signals using optical means.

The relative SOPs remained sufficiently stable through a few minutes-long data acquisition. Polarization stability would benefit from the use of shorter fiber sections, and from more advanced electronic processing, leading to faster data acquisition. The polarization alignment sequence described in section 3 is simple and reproducible. Further work would lead to the automation of the alignment procedure.

The high resolution and accuracy of the measurement scheme would depend on pump frequencies monitoring and calibration, and on fixed frequency offsets among the pump lines. To that end, a broadband MZM could generate both the SBS gain pump and the SBS loss pumps from the output of a single source, and guarantee the stability of their frequency differences. We have employed this technique in an earlier work [30]. This arrangement would also promote the alignment of the pumps SOPs, and reduce the number of independently aligned PCs to two.

The extension of the spectral measurement range beyond a few tens of GHz cannot rely on the sweeping of modulation sidebands alone. Widely tunable laser diode sources would have to be used instead. Since the frequencies of tunable lasers are not perfectly repeatable, certain measures for referencing and stabilization would be necessary [10, 31, 32]. Alternatively, an array of DFB lasers, with precise current and temperature control, may be used to cover a broad spectral range. The method is restricted to the measurement of a single polarization component of the signal under test. The two individual components of polarization-multiplexed waveforms may be measured separately, using a properly aligned input polarizer. Lastly, we note that SBS-based polarization pulling is also underlying recent demonstrations of sharp and tunable optical band-pass filters [20] and of advanced modulation formats [33]. The principle may also be applicable to the enhancement of quasi-light storage, based on SBS [34, 35].

Acknowledgments

The authors wish to thank Dr. Kambiz Jamshidi and Jens Klinger from the Institut für Hochfrequenztechnik, Hochschule für Telekommunikation, in Leipzig, Germany, for their assistance in the experimental work. SP and AW acknowledge the financial support from the Deutsche Telekom Laboratories. The work of AZ was supported in part by the German-Israeli Foundation (GIF), under Grant No. I-2219-1978.10/2009. TS acknowledge the support from the Deutsche Forschungsgemeinschaft (DFG), under Grant No. SCHN 716/6-2. The collaboration of AZ and MT is within the European Cooperation on Science and Technology (COST) Action TD1001.

#165286 - $15.00 USD Received 23 Mar 2012; revised 10 May 2012; accepted 12 May 2012; published 15 Jun 2012